Strain-based formulas for stresses in profiled center-wound rolls

S. J. BURNS, RICHARD R. MEEHAN, AND J. C. LAMBROPOULOS

ABSTRACT

A new solution to the problem of modeling elastic stresses in center-wound rolls is proposed. Its premise is that residual strains from the web relax to create stresses within the roll. Stress terms—obtained with linear and nonlinear elastic solutions—are weighted averages of web stresses in center-wound rolls. However, there are major differences between these calculated stresses and previous solutions. The solution here rigorously satisfies two boundary conditions and is in closed form. The proposed approach contains four stress terms: Two are general stresses from the homogeneous part of the solution, while two new solutions come from the residual strains in the roll generated by web tension stresses. The radial dependence of the residual strains (i.e., the roll profile) is very important, since the residual roll stress depend on the winding conditions. All winding profiles lead to complete, although algebraically complicated, elastic solutions in analytic form. Nonlinear elastic solutions are also investigated using the effective residual web stress and a stress-dependent radial elastic modulus. Numerical nonlinear equations developed from expressions derived here have straightforward solutions. A selection of material constitutive laws and roll profiles are evaluated for comparison. Finally, the modeled roll stresses are compared with pull-tab-measured stresses from instrumented wound rolls. The radial plateau stresses in the midroll are further approximated with several simple closed-form algebraic expressions.

Application:

A new approach for modeling the elastic stresses in center-wound rolls.

CENTER-WOUND ROLLS ARE A convenient, compact storage scheme for web products. However, the stresses in rolls can cause damage, especially in tightly wound rolls that are stored for a long time. The objective in creating a roll is to select parameters in the web, hub, and roll that profiles the stresses for minimum damage to the medium while avoiding cinching, spoking, telescoping, or soft-hub roll buckling.

The stresses in center-wound rolls are essential to the integrity of the roll. Consequently, these stresses have been the subject of theoretical and experimental studies for at least the last 30 years *(1–8)*. They were initially modeled by assuming a cylindrically symmetric geometry for the center-wound roll that is mechanically loaded on the outermost wrap. This layer is considered a hoop stress, at the web tension, on the outer wrap as the roll is constructed layer by layer. Early work by Altmann *(1)* provided a general solution for an anisotropic linear elastic roll material while using a nonlinear constitutive relation to find the radial and hoop stresses for successive wraps. The nonlinear constitutive laws attempt to account for interlayer contacts, material discontinuities, and anisotropic intralayer wraps in the roll.

Altmann *(1)* solved a second-order differential equation for the anisotropic linear elastic material in a center-wound roll. He introduced to his solution an outer wrap described by a parabolic radial stress–strain relation, i.e., the modulus was proportional to the stress. Boutaghou and Chase *(2)* noted that Maxwell's equations (from elastic energy function arguments) reduce the number of independent terms in Altmann's elastic constants. They also found some general properties of center-wound rolls with anisotropic linear elastic media. Yagoda *(3)* established the core compliance as an inner boundary condition on center-wound rolls. The constitutive relations for stacked sheets were examined by Pfeiffer *(4)* and Olive *(9)*, who suggested empirical forms for stress vs. strain. A general nonlinear power-series constitutive law was alternatively used by Hakiel *(5)*. The first term of Hakiel's series is related to one of Pfeiffer's *(4)* material constants. Hakiel incorporated nonlinear material properties into his expressions of the basic mechanics and numerical solutions of wound-roll stresses.

Good *et al.* *(6)* compared results from Hakiel's model with interlayer pressure measurements obtained using pull tabs. They noted that the model typically predicted stresses that were twice as large as their measured values. However, they were able to bring predicted and measured values into better agreement by modifying the outer hoop-stress boundary condition to relax relative to the outer-layer tensile stresses by their model of "wound on tension" loss. Benson *(8)* later showed that a large-strain, nonlinear constitutive law that accounted for hoop-stress relaxation gave agreement between the predicted interlayer pressures and measurements without additional assumptions about wound-on-

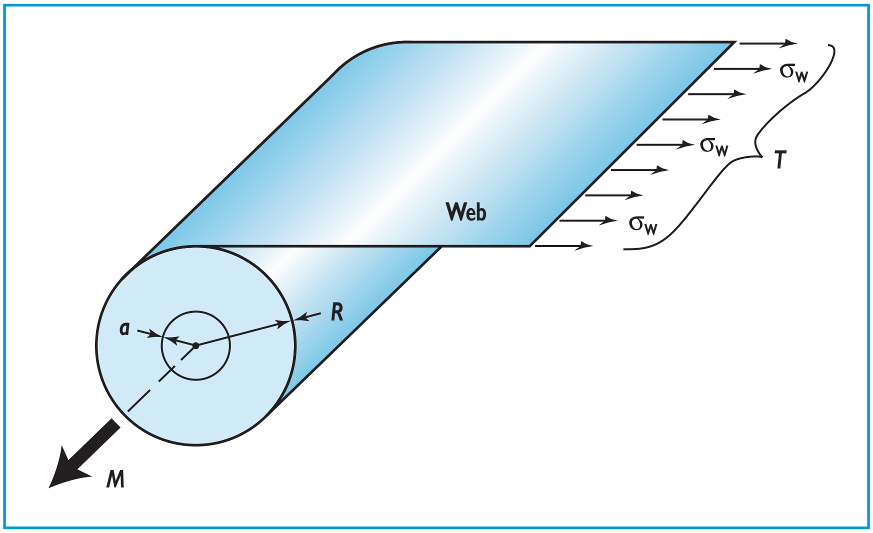

1. Schematic representation of a center-wound roll with the geometry described in the text. The force* T *acting on the roll creates the web stress σ_w, and the hub torque* M *winds the roll.

tension losses. The roll's hoop stresses in these models might be thought to be equated to the web stress, provided there is little or no friction between layers. Air entrained in the roll would also aid in equalizing these stresses *(10)*. On the other hand, the "belt wrap" equation from elementary mechanics predicts that interlayer friction would quickly lower web stresses and the intralayer stress in the outermost wrap of the roll.

After reviewing the literature, it is clear that the second-order differential equation for the stresses in the center-wound roll is assumed initially to satisfy two boundary conditions:

1. Continuity of radial stresses and displacements between the hub and the roll. (Thus the hub compliance is incorporated into the roll stress.)
2. Zero radial stress on the outer wrap of the roll.

Finally, the hoop stress on the outer wrap is often equated to the web stress during the lap-by-lap construction of the roll. Clearly, this latter condition would overspecify the number of arbitrary constants in the differential equation's solution. It calls into question whether the hub compliance is indeed constant in numerical solutions of center-wound-roll stresses. The numerical solutions are constructed in a lap-by-lap analysis while building up stresses in the roll from the hub outward.

In this paper, the assumption that the hoop stress in the outer wrap is equal to the web tension stress is removed. Instead, residual strains in the web are wound onto the roll, where they are relaxed and equilibrated. The elastic stress solutions found here use the residual strains placed in the roll by the web, assuming the wraps do not slip. The residual strains from the web thus create the roll's stresses. The radial and hoop directions are principal stress directions, so there are no shear stresses between the web and the first layers in the roll. The hoop stresses on the outside of the roll, as developed here, are completely unspecified except for residual strains. In the stress analyses of center-wound rolls, the hoop and radial stresses have always been considered principal stresses *(1–8)*, and interlayer friction has not been specified. In reality, friction and adherence between the wraps of the roll and the stresses created are probably important. Thus, the strain model developed here and previous stress models are only two limits of a more complex problem.

This paper takes a new approach by modeling the center-wound roll in terms of the residual wound-on strains that are initially in the web. The proposed model posits that these strains are spooled onto the roll and create all the stresses within the roll. Thus the roll's stresses come from the web's state of strain, which can be profiled as residual strains in the roll. The analysis of the roll's stresses is consistent with the equations of solid mechanics for linear and nonlinear elastic materials. Although the stresses found here are very different from those cited in the literature *(1–9)*, there are some close similarities with conventional center-wound-roll expressions.

MODEL OF A CENTER-WOUND ROLL

Figure 1 is a schematic geometry of the tension T acting on the web and roll. A torque M is applied to the hub to wind the roll. Moment equilibrium gives $M = RT$. It follows that the work done by T from a displacement ds of the moving web is exactly balanced by the work done by angular rotation, $d\phi$, of M on the hub, since $Rd\phi = ds$. Thus the net increase in the strain energy of the wound roll, which is the difference between these work terms, is effectively zero. The model is that the strain energy deposited into the roll derives from the residual strain energy in the web. The stresses from the mechanical action of the force T on the roll are typically very small, and such stresses would be removed when T is set to zero after winding.

ANALYSIS OF RESIDUAL ROLL STRESSES CREATED BY RELAXATION OF WEB STRAINS

The strains in a web are spooled onto a center-wound roll lap by lap. These residual strains are only part of the total strains within the roll. However, when they relax, they create stresses in the roll that can be very large. These residual stresses are the subject of this paper.

The cylindrical symmetry of the roll implies that the radial displacement u is the only displacement component and is only a function of the radius r, i.e., $u = u(r)$. The total strains in the roll are split into two components: One is assumed to be elastic and comes from the stresses, while the other is from the residual strains that are directly transferred to the roll from the web. The elastic strains are designated as ε_{ij}, and the residual strains are ε^*_{ij} for the radial (Eq. 1) and hoop (Eq. 2) directions.

$$\frac{\partial u}{\partial r} = \varepsilon_{\mathrm{rr}} + \varepsilon^*_{\mathrm{rr}} \qquad (1)$$

$$\frac{u}{r} = \varepsilon_{\theta\theta} + \varepsilon^*_{\theta\theta} \qquad (2)$$

The terms on the left side of Eqs. 1 and 2 represent the total strain. The first term on the right is the elastic strain. The second term on the right is the residual strain, which is the difference between the relaxed state (no strain) less the state of strain in the web before it is spun onto the roll. Substituting Eq. 2 into Eq. 1 provides compatibility for the strains ε_{ij} in the two principal stress directions.

$$r\frac{\partial \varepsilon_{\theta\theta}}{\partial r} + \varepsilon_{\theta\theta} - \varepsilon_{\mathrm{rr}} = \varepsilon^*_{\mathrm{rr}} - \frac{\partial (r\varepsilon^*_{\theta\theta})}{\partial r} \qquad (3)$$

Initially, the strains will be assumed to be linear in stress. Nonlinear elastic stress solutions are addressed later. The linear elastic strains in the roll are related to the stresses by Hooke's law:

$$\varepsilon_{\mathrm{rr}} = s_{11}\sigma_{\mathrm{rr}} + s_{12}\sigma_{\theta\theta} + s_{13}\sigma_{zz} \qquad (4)$$

$$\varepsilon_{\theta\theta} = s_{12}\sigma_{\mathrm{rr}} + s_{22}\sigma_{\theta\theta} + s_{23}\sigma_{zz} \qquad (5)$$

$$\varepsilon_{zz} = s_{13}\sigma_{\mathrm{rr}} + s_{23}\sigma_{\theta\theta} + s_{33}\sigma_{zz} \qquad (6)$$

where σ_{ij} represents the stresses. The s_{ij} variables are the elastic compliances and, in an anisotropic elastic solid, they are symmetric from Maxwell's relations, so $s_{ij} = s_{ji}$. It has been assumed that the deformation is completely radial, so the stresses and strains are principal components, with all shear stresses in these coordinates zero. The stress components for plane strain assume $\varepsilon_{zz} = 0$, while plane stress has $\sigma_{zz} = 0$. The solution here is for plane strain, so in what follows, set $s_{23} = s_{13} = 0$ in Eqs. 4–6 for plane stress. Finally, force equilibrium is maintained between the radial- and hoop-stress components. It follows that

$$\sigma_{\theta\theta} = (1 + D)\,\sigma_{\mathrm{rr}} \qquad (7)$$

The operator $D \equiv [r(d/dr)]$ simplifies the following expressions and permits r for the remainder of this discussion to be dimensionless. Thus r is a radius ratio, i.e., the radius divided by the hub radius a.

Substituting Eqs. 6 and 7 into Eqs. 4 and 5 and collecting terms in Eq. 3 gives a differential equation for the stress, σ_{rr}.

$$\left[D^2 + 2D + (1-\beta^2)\right]\sigma_{\mathrm{rr}} = \sigma^*(r) \qquad (8)$$

where

$$\beta^2 = \frac{s_{11}s_{33} - s_{13}^2}{s_{22}s_{33} - s_{23}^2} \qquad (9)$$

and

$$\sigma^*(r) = \frac{s_{33}\left\{\frac{1}{E_{22}}\frac{d}{dr}\left[r\sigma_{\mathrm{w}}(r)\right] + \frac{\nu}{E_{22}}\sigma_{\mathrm{w}}(r)\right\}}{s_{22}s_{33} - s_{23}^2} \qquad (10)$$

Note that for most wound flexible media, $\beta^2 > 1$. To find the residual stress in the roll $\sigma^*(r)$, use the right side of Eq. 3 with Eqs. 11a or 11b:

$$\varepsilon^*_{\theta\theta}(r) = -\frac{1}{E_{22}}\sigma_{\mathrm{w}}(r) \qquad (11a)$$

$$\varepsilon^*_{\mathrm{rr}}(r) = \frac{\nu}{E_{22}}\sigma_{\mathrm{w}}(r) \qquad (11b)$$

The web stress $\sigma_{\mathrm{w}}(r)$ creates the roll's residual strains. However, the web's elastic constants are not necessarily the same as those in the roll. Consequently, the proposed model uses the web's E_{22} and ν instead of the roll's elastic compliances, s_{22} and s_{12}.

The effective characteristic residual stress in the roll, $\sigma^*(r)$, is from the web's strains and, in a restricted limit, is the web tension. In general, $\sigma^*(r)$ depends on roll radius through the web tension as the outer layer is placed onto the roll. Thus this stress depends on the roll radius ratio and on how the roll is profiled. Finally, s_{22}, s_{33}, and s_{23} in Eq. 10 are elastic compliances relating the strains in the web to the residual stress, $\sigma^*(r)$, in the roll.

The solution to Eq. 8 is the stress σ_{rr} in the wound roll. The solution is given in Eq. 12.

$$\sigma_{\mathrm{rr}} = \left(\frac{A}{r^{1+\beta}} + \frac{B}{r^{1-\beta}}\right) + \frac{1}{2\beta r}\left[r^{-\beta}\int_r^R t^{\beta}\sigma^*(t)\,dt - r^{\beta}\int_r^R t^{-\beta}\sigma^*(t)\,dt\right] \qquad (12)$$

The homogeneous solution contained in Eq. 12 incorporates two arbitrary constants, A and B. The particular solution to the differential equation is found using Lagrange's method of variation of parameters *(11)*. The lower limit in the integration was used for r, since this choice facilitates direct comparison with Altmann's and subsequent work on stresses in center-wound rolls *(1-9)*.

The first boundary condition is that the outside of the roll is stress free, or $\sigma_{\mathrm{rr}} = 0$ when $r = R$. Thus Eq. 12 can be recast as Eq. 13.

$$\sigma_{\mathrm{rr}} = \frac{1}{r}\left\{\left[B\left(r^{\beta} - \frac{R^{2\beta}}{r^{\beta}}\right)\right] + \frac{1}{2\beta}\left[r^{-\beta}\int_r^R t^{\beta}\sigma^*(t)\,dt - r^{\beta}\int_r^R t^{-\beta}\sigma^*(t)\,dt\right]\right\} \qquad (13)$$

Data set	No. 2	No. 3	No. 4	No. 5	No. 6
Literature citation	*(5)*	*(5)*	*(6)*	*(6)*	*(16, 17)*
Figure	Fig. 2	Fig. 3	Fig. 4	Fig. 4	Fig. 5
Material	Polyester (PET)	Resin-coated paper	Newsprint	Newsprint	Polyester (PET)
Thickness, µm	76	230	89	71	15.7
Poisson's ratio of the web (ν)	0.28	0.01	0.01	0.01	0.28
Web stress (σ_w), MPa	2.30	3.83	5.17	5.17	5.09
Radial compliance (s_{11}), 1/MPa	1/690	1/34.2	nonlinear only	1/14	1/145
Nonlinear radial coefficient (α)	linear	linear	65.2	50.6	695
Hoop compliance (s_{22}), 1/GPa	1/4.14	1/4.14	1/4.13	1/3.37	1/3.79
Hub core stiffness (E_c), GPa	6.14	6.14	12.4	33.1	30.4
Outer roll radius ratio (R)	4	2, 3, 4, and 5	2	3	3.11

Note:
z-axis plane-strain compliance (s_{33}) = hoop compliance (s_{22}) = 1/Young's modulus of the web
Poisson compliance (s_{23}) = $-\nu\, s_{22}$

I. Physical properties of roll and web media

The hoop stress follows from Eq. 7 and is given by Eq. 14.

$$\sigma_{\theta\theta} = \frac{1}{r}\left\{\left[\beta B\left(r^{\beta} + \frac{R^{2\beta}}{r^{\beta}}\right)\right] - \frac{1}{2}\left[r^{-\beta}\int_r^R t^{\beta}\sigma^*(t)\,dt + r^{\beta}\int_r^R t^{-\beta}\sigma^*(t)\,dt\right]\right\} \tag{14}$$

The second boundary condition relates the effective hub compliance, i.e., the hub displacement divided by the radial stress, to the wound roll's values at the interface where r = 1. Quantitatively, the radial stresses and the displacement of the hub equal those in the roll. This expression is evaluated using Eqs. 2, 5, 13, and 14. This second boundary condition uniquely determines the arbitrary constant B.

$$\left.\frac{u}{r\sigma_{rr}}\right|_{hub} \equiv \frac{1}{E_c} = \left.\frac{u(r=1)}{\sigma_{rr}(r=1)}\right|_{roll} \tag{15}$$

which for plane-strain conditions gives Eq. 16: (see below)

The roll stresses are therefore known in closed form for the general case of any web stress profile. Note that B as given here depends on R. This implies that the solutions in the literature *(1–8)* should include adjustments to the inner boundary condition as laps are wound onto the roll.

LINEAR ELASTIC STRESSES IN CENTER-WOUND ROLLS

Several examples of linear elastic center-wound rolls are presented based on data from the literature, which are provided in **Table I**. **Figure 2** shows the stresses for three common winding conditions: constant web tension, constant torque on the hub, and a web tension that is linearly profiled from the hub to the outside of the roll (with a one-third reduction in web tension). Comparison of Figs. 2a and 2b shows that in each case, the values of $\sigma^*(r)$ from Eq. 10 are not identical to the web stress $\sigma_w(r)$. Note that $\sigma^*(r)$ includes a Poisson effect in the web from through-the-thickness strains in the web. Such strains are easily envisioned. However, the Poisson effect in the roll is quite different. In the roll, this effect is generally thought to be small and is often set to zero *(1–8, 12, 13)*. Here, s_{12} is unspecified, since it does not appear in Eqs. 8–10. Note that the stresses in the roll are from the *differences* in the principal residual strains in the roll. Thus, both strains in the web add directly to the residual strains and thus to the stresses in the roll. For the latter two profiled rolls, and for ease of comparison at the very start of winding, $\sigma_0 \equiv \sigma_w(r=R=1)$. The characteristic residual stress $\sigma^*(r)$ profiles are shown in Fig. 2b. The roll stress $\sigma_{rr}(r)$ was evaluated from the general expressions in Eqs. 13–16. The winding conditions in the following Examples 1–3 assume linear elastic stresses with profiled $\sigma^*(r)$ functions.

Example 1: Constant web tension

The first linear elastic example is for constant web tension, i.e., σ_w = constant.

$$\frac{\sigma^*(r)}{\sigma_0} = C$$

$$C = s_{33}\left(\frac{\frac{1}{E_{22}} + \frac{\nu}{E_{22}}}{s_{33}s_{22} - s_{23}^2}\right) \tag{17}$$

$$B = \frac{-\left\{-2\beta\sigma_w(r=1)E_c s_{22} + \left\{\left[E_c(s_{12}-\beta s_{22})-1\right]\int_1^R t^{\beta}\sigma^*(t)\,dt\right\} + \left\{\left[1-E_c(s_{12}+\beta s_{22})\right]\int_1^R t^{-\beta}\sigma^*(t)\,dt\right\}\right\}}{2\beta\left[(R^{2\beta}-1)(1-s_{12}E_c)+\beta E_c s_{22}(1+R^{2\beta})\right]} \tag{16}$$

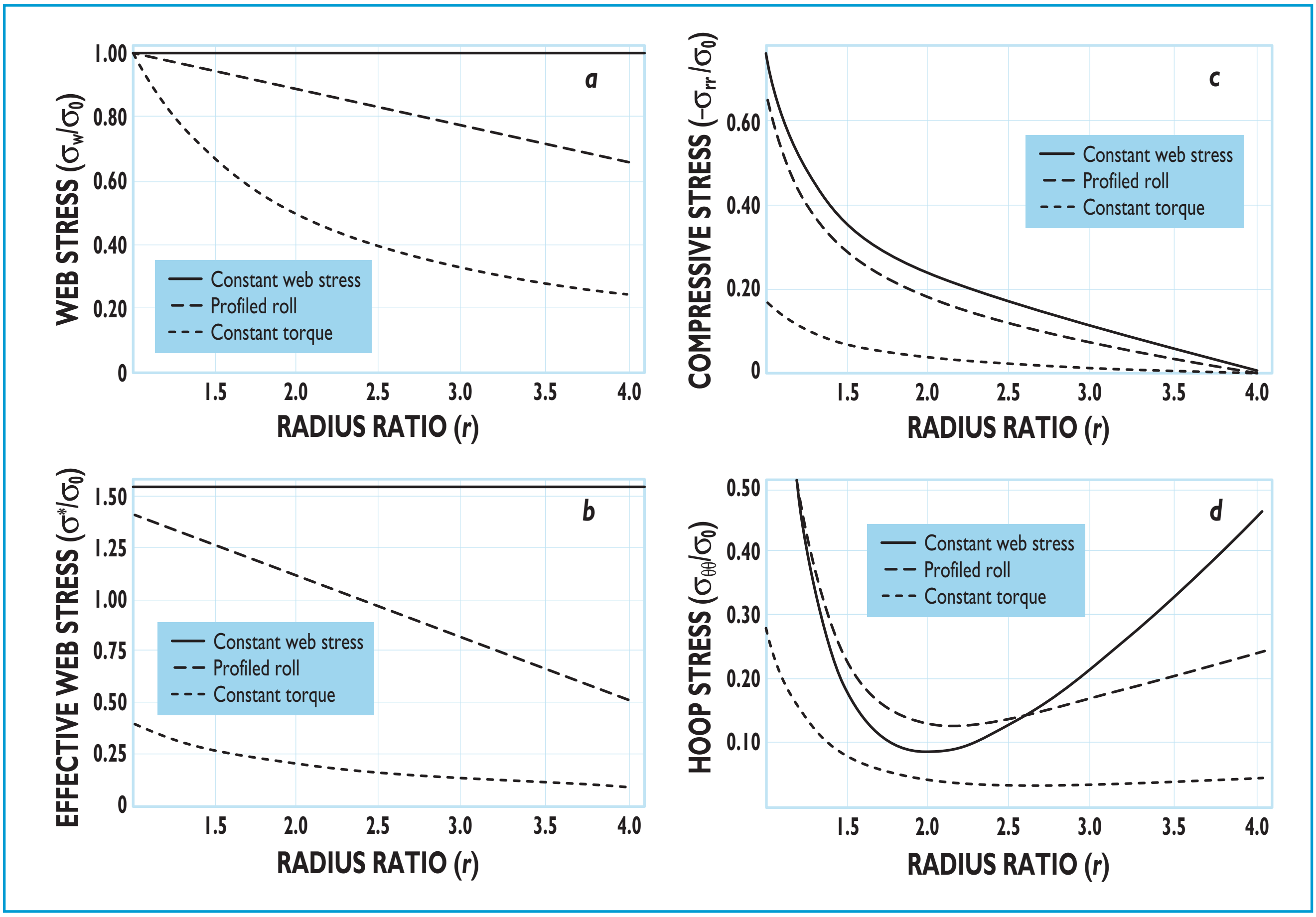

2. Stresses—a: web stress, b: effective web stress, c: radial compressive stress, and d: hoop stress—vs. roll radius in profiled linear elastic center-wound rolls (experimental details in Table I)

where if all Poisson effects $\Rightarrow 0$, then $C \Rightarrow 1$

Example 2: Constant torque on the roll's hub

The second linear elastic example is for constant torque M on the roll's hub, with $r\sigma_w(r) \propto rT$, which is constant and proportional to M.

$$\frac{\sigma^*(r)}{\sigma_0} = \frac{\nu}{rE_{22}s_{22}} \quad (18)$$

Example 3: Linear taper in web tension

The third linear elastic example is for a linear taper in web tension, with a 33% reduction in tension from the hub to the outside of the roll:

$$\sigma_w(r) = \frac{\sigma_0(3R - 2 - r)}{3(R-1)}$$

so

$$\frac{\sigma^*(r)}{\sigma_0} = C\left[\frac{(1+\nu)\,(2-3R+r)+r}{3(R-1)}\right] \quad (19)$$

Figure 2c shows the roll's radial stress plotted as a compressive stress, i.e., $-\sigma_{rr}/\sigma_0$, for the three profiles. Figure 2d shows the hoop stress, $\sigma_{\theta\theta}/\sigma_0$. Note that in all cases, σ_{rr} and $\sigma_{\theta\theta}$ are both linear elastic stresses, so they scale with the amplitude of σ_w. The solutions seen in Fig. 2 differ from linear elastic solutions in the literature as follows: The effective stress, $\sigma^*(r)$, is not necessarily equal to the web stress, σ_w, even for constant web stress. In this case, σ^*/σ_0 is greater than 1 because this is a plane-strain solution and, in addition, there is a Poisson effect in the web that contributes to σ^*. The σ^* for the constant-torque roll is much less than for the profiled roll because $r\sigma_w$ is constant, so the first term on the right in Eq. 10 is zero. Finally, the compressive stresses near the hub are flatter than similar stresses seen in the literature in center-wound rolls.

Example 4: Radial and hoop stresses with changing roll radius

The fourth linear elastic example shows $-\sigma_{rr}/\sigma_0$ and $\sigma_{\theta\theta}/\sigma_0$ while letting R change with the winding tension. The stresses are shown in **Fig. 3**. The roll properties and winding conditions are given in Table I (Data Set 3). The plots are for R equal to 2, 3, 4, and 5. The value of $\beta \approx 11$, so a broad plateau develops in the roll, especially at large R.

NONLINEAR ELASTIC STRESSES IN CENTER-WOUND ROLLS

In the literature, even in the earliest papers, it was assumed that the radial modulus should reflect the asperities and interfacial contacts between the

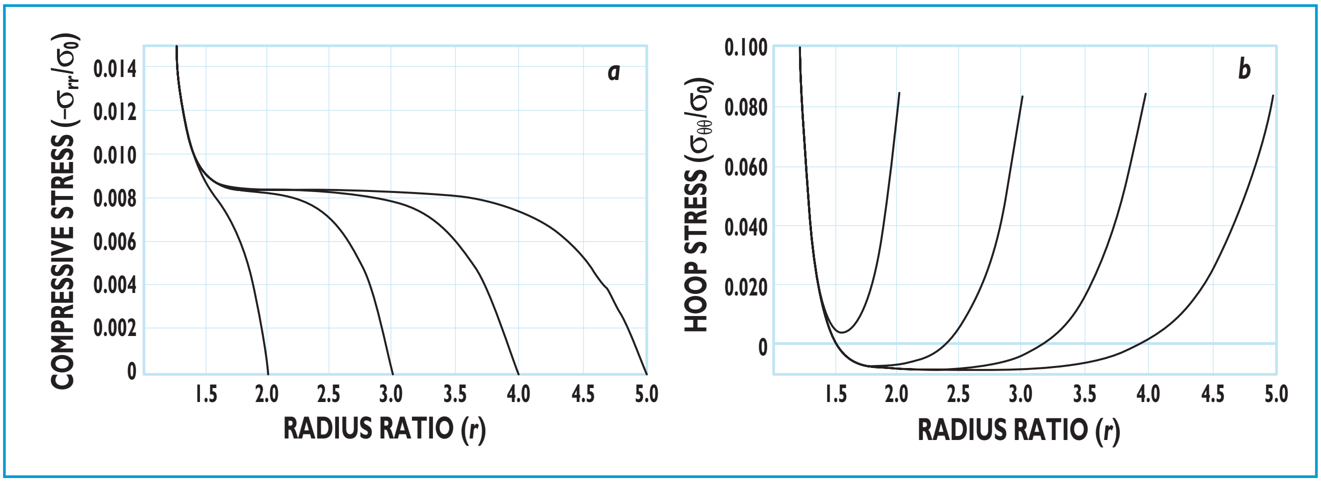

3. Stresses—a: radial compressive stress and b: hoop stress—vs. roll radius in a center-wound roll at constant web tension for linear elastic media with outer-roll radii ratio ranging from 2 to 5 (experimental details in Table I)

layers of the roll. Thus, the radial modulus for center-wound-roll media is widely represented by a nonconstant, nonlinear expression. The constitutive law is typically obtained by curve-fitting the load per unit area vs. strain for a stack of sheets *(4, 12–14)*. The derivative of this stress with respect to the strain is the radial modulus as a function of the strain. The stress and modulus vs. strain are parametric equations solved for modulus vs. stress. Frequently, the modulus is reported to be proportional to the compressive stress, as assumed in the following analysis.

The more complex problem of a constitutive law for a biaxially or triaxially stressed stack during loading (and unloading) is typically not addressed. If it is assumed in Eqs. 8–10 that all Poisson ratios in the roll are zero and that the modulus is proportional to the pressure (i.e., the negative stress), then

$$E_r = -\alpha\,\sigma_{rr} = \frac{1}{s_{11}}$$

so

$$(D^2 + 2D + 1)\,\sigma_{rr} = \sigma^*_{n-\ell}(r) \qquad (20)$$

where the nonlinear characteristic stress $\sigma^*_{n-\ell}(r)$ is

$$\sigma^*_{n-\ell}(r) = \frac{1}{\alpha s_{22}} + \left\{\frac{d}{dr}\left[r\,\sigma_w(r)\right] + \frac{\nu}{E_{22}s_{22}}\,\sigma_w(r)\right\}$$

This nonlinear modulus must be used in compression. Such a modulus, of course, would be unstable were the stresses to change sign.

The solution to Eq. 20—after eliminating one arbitrary constant (by satisfying the boundary condition $\sigma_{rr} = 0$ at $r = R$)—is shown in Eq. 21.

$$\sigma_{rr} = \frac{B_1}{r}\,\ell n\!\left(\frac{r}{R}\right) + \frac{1}{r}\left[\int_r^R \ell n(t)\,\sigma^*_{n-\ell}(t)\,dt - \ell n(r)\int_r^R \sigma^*_{n-\ell}(t)\,dt\right] \qquad (21)$$

The hoop stress follows from Eqs. 7 and 21, as seen in Eq. 22.

$$\sigma_{\theta\theta} = \frac{B_1}{r} - \frac{1}{r}\left[\int_r^R \sigma^*_{n-\ell}(t)\,dt\right] \qquad (22)$$

B_1 is found using Eq. 15, which was evaluated with the aid of Eqs. 2, 5, 21, and 22. The expression for B_1 is given in Eq. 23.

$$B_1 = \frac{\int_1^R \ell n(t)\,\sigma^*_{n-\ell}(t)\,dt + E_c s_{22}\left[\sigma_w(r{=}1) + \int_1^R \sigma^*_{n-\ell}(t)\,dt\right]}{\ell n(R) + E_c s_{22}} \qquad (23)$$

Thus the stresses σ_{rr} and $\sigma_{\theta\theta}$ are uniquely obtained for any winding profile. The stresses σ_{rr} and $\sigma_{\theta\theta}$ are shown in **Fig. 4** for the nonlinear web parameters listed in Table I (Data Sets 4 and 5). The winding profile is constant web tension, as noted previously. The stresses developed in the roll are quite large because the effective web stress $\sigma^*_{n-\ell}$ is large. The value of $1/(\alpha s_{22})$ is 12.1 and 15.6 times the web stress for $R = 2$ and 3 rolls, respectively. The very large value of $\sigma^*_{n-\ell}$ elevates all the stresses in the roll, with the stresses being high compared with pull tabs *(6)*.

ESTIMATES OF PLATEAU STRESSES IN THE ROLL

The previously derived stresses are predictions using elastic solutions that satisfy well-defined boundary conditions. However, the experimentally measured stresses in center-wound rolls typically show a broad plateau of nearly constant stress over most of the roll *(5–8)*. If it is assumed that the radial stress is constant throughout the roll, then Eq. 7 dictates that the hoop stress equals the radial stress. The web's elastic strain energy density for this case is then equal to the roll's linear elastic strain energy density. Equating these energies and solving for the radial stress in the roll gives Eq. 24.

$$\left|\sigma_{rr,\,avg}\right| \approx \frac{\sigma_w}{\sqrt{2(1 + s_{11}E_{22})}} \qquad (24)$$

The stresses seen in the proposed model and in other models of center-wound rolls are generally larger at the hub and smaller on the

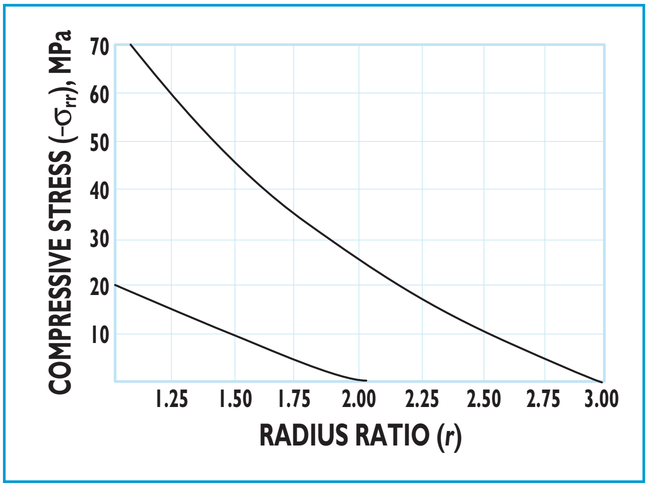

4. Radial stresses vs. roll radius in a center-wound roll assuming nonlinear elastic properties for the layered roll media (experimental details in Table I)

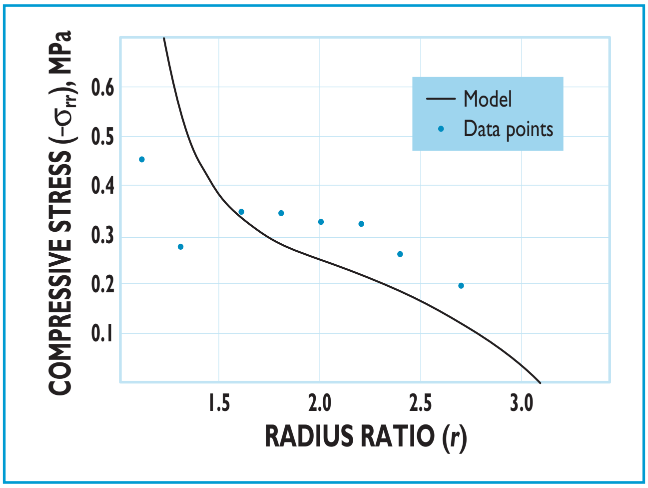

5. Comparison of calculated radial stresses and measured pull-tab data (16) that have been corrected for stress concentrations (15) (experimental details in Table I)

outer laps. Equations 12–14 show that these two boundary conditions are represented by $r^{\beta-1}$ and $1/r^{\beta+1}$, respectively. The large hub strain energy very roughly cancels with the smaller strain energy on the outside of the roll in the approximation of Eq. 24. Typically, $\beta^2 >> 1$, so the right side of Eq. 24 is approximately $\sigma_w/\sqrt{2\beta}$. Thus the stress in the roll is significantly reduced compared with the web stress in this rough but very simple approximation. Pfeiffer *(4)* reported a similar expression aside from $\sqrt{2}$.

Nonlinear elasticity in the roll can be incorporated into Eq. 24 by finding the area under the stress-vs.-strain or load-vs.-displacement curve for the media, i.e., the strain energy density in the layered roll media. This strain energy density would be found as a function of stress and equated to the web's strain energy density. The approximation is that the strain energy density in the roll is a constant.

Finally, the stresses in the analytic equations with constant web stress always reduce to a very simple form in numerical expressions for the stresses. It has only three terms: a constant, a term proportional to $1/r^{\beta+1}$, and a third term proportional to $r^{\beta-1}$. The interpretation here is quite simple, with the two r terms representing the solutions of the inner and outer boundary conditions, respectively, as noted previously. If β is very large, then these two terms nearly become step functions. The constant term is the radial plateau stress. This is seen in the midsection of the wound rolls in Fig. 3, which depicts compressive and hoop stresses under constant web tension.

Equating the constant stress term in Eq. 13, i.e., a stress that is independent of r, to a plateau stress represents the midstress shown in Fig. 3. Plateau stresses are widely measured in center-wound rolls *(1, 5, 6)*. The lower limit of the two integrals on the right in Eq. 13 are independent of the roll radius ratio for constant web stress. The following algebraic expression is obtained after evaluating these integrals. The roll's plateau stress is given by Eq. 25a.

$$\sigma_{rr,\ plateau} = \frac{\sigma^*(r)}{1-\beta^2} \tag{25a}$$

so

$$\sigma_{rr,\ plateau} \approx -\frac{\sigma^*(r)}{s_{11}E_{22}} \tag{25b}$$

The plateau stress can also be obtained directly from the differential Eq. 8 by assuming the stress to be constant, thus converting all derivatives to zero and reducing Eq. 8 to Eq. 25a. In Fig. 3, where $\beta \approx 11$, the plateau stress is in agreement with Eq. 25b. Furthermore, a constant radial plateau stress implies that the hoop stress is equal to the radial stress, as discussed previously and also seen in Fig. 3. Thus, a plateau stress implies that the hoop stress is in compression and is constant.

Good *et al. (6)* presented a figure (Fig. 6 in their work) that predicts that plateau stresses from Hakiel's model *(5)* are proportional to σ_w. Equation 25 shows that $-\sigma_{rr}$ is directly proportional to $\sigma^*(r)$ with a slope of $1/(\beta^2-1)$. Furthermore, $-\sigma_{rr}$ is approximately proportional to $1/s_{11}$, i.e., to E_r, when $\beta^2 > 1$, which is typical for center-wound media. Thus, $-\sigma_{rr}$ is proportional to E_r, which itself may depend on σ_{rr}. Equation 25 was suggested in the work of Good *et al. (6)* from numerical solutions of Hakiel's nonlinear stress models *(5)* with a wide selection of E_r and σ_w values for a specific material. The slope from Eq. 25 vs. $1/s_{11}$, i.e., E_r, is σ^*/E_{22}, which is smaller than suggested by the work of Good *et al. (6)*. Thus, Eq. 25 is in agreement with the form of the nonlinear model but not with the individual calculated values from the work of Good *et al. (6)*. The more important comparison is to measured plateau stresses from pull-tab data *(15, 16)*. This comparison is presented in **Fig. 5** and is discussed in the following section.

DISCUSSION AND CONCLUSIONS

Elastic stress solutions in center-wound rolls have been presented using the concept of relaxing the residual strains placed in the roll. The basic model is that the wraps laid on the roll do not slip and that the residual strains from the web create the roll's stresses. The homogeneous solution for these stresses is already known, while the particular solutions found here are based on mathematical solutions to differential equations. The particular solutions are weighted averages of the residual stresses when they are spooled onto the roll from the web. Part of this solution agrees with the physically intuitive stress model of the outer wraps placed on the roll. The particular solution, however, is an average of weighted stress terms that are not totally intuitive but are needed for the complete mathematical solution of the second-order differential equation. These solutions contribute to the inner boundary condition.

A final comparison is now made between recent data *(16)* and the proposed strain-based model. The recent data *(16)* were corrected for stress concentrations associated with the sandwiched pull tabs *(15)*. The linear model in Fig. 5 was applied using a nonlinear modification that was found with the following procedure:

1. Plateau stress is obtained from Eq. 25a using the complete elastic properties, including all the nonlinear parts of radial elastic modulus, $1/s_{11}$.
2. The radial elastic modulus, $1/s_{11}$, is then determined at the obtained value for plateau stress.
3. Roll stress vs. roll-radius ratio is then determined at the obtained value for plateau stress using Eqs. 13, 14, and 16 and the elastic constants found in Step 2.

The nonlinear elastic constitutive law is explicitly included in the stress solution given above. The data are from compression loading of stacked layers of media. The constitutive law from load-vs.-displacement curves typically emphasizes the high part of the curve rather than low stresses. This can lead to very large differences in the constitutive law. Our experience has led to differences as large as 300% in the major terms in the nonlinear constitutive law. However, unloading may better represent the elastic compliances necessary to describe stresses in the roll. Comparison between the model and the data in Fig. 5 shows that the value of β used in the model does not bring the analytic stresses up as sharply on the outside of the roll as the experimental data suggest. Moreover, the stresses measured near the hub are smaller than predicted by the analytic curve, again indicating that the value of β used in the analytic expression is too small. The plateau stress depicted by the model is in modest agreement with the experimental data.

The stress solutions presented have been constructed to be similar to the elastic solutions in the literature. However, the solutions would be simpler if the integrals in the particular solution were chosen to go from $1 \Rightarrow r$ rather than from $r \Rightarrow R$. This change would significantly simplify the inner boundary condition while only slightly complicating the outer one. As long as numerical solutions are obtained, then either method works. Simple analytic solutions using the hub core as the lower limit in the particular solutions might provide some additional physical insights.

The expressions for $\sigma^*(r)$ found here rely on compatibility relations between displacements and their derivatives to obtain the strains. Additional terms contributing to the stress $\sigma^*(r)$ come from the shape of the roll's profile. If the roll is profiled with a constant-torque winding, then most of the radial derivatives of the residual strains are removed. The roll stresses presented here show that constant-torque rolls have a unique characteristic: In linear elastic media, the web stress does not directly contribute to the roll's stresses, and the Poisson effect in the web (not in the roll) is the only contributor to the roll's stress. In general, the residual strains in the roll are from the differences in the principal web strains, so Poisson's effect in the web adds to the roll's stresses. It also follows that the roll's stresses scale with the maximum residual shear strains in the web. Shear stresses are the major contributor to plastic deformation and damage, such as viscoelastic behavior in the roll. Thus these effects are directly related to the differences in the web's principal strains. Interlayer adhesion responds to the stresses σ_{rr}, which for linear elastic materials also scales with the difference in web strains.

The simplest nonlinear radial modulus has a term that is proportional to the radial stress. This stress-dependent modulus gives rise to an equivalent web strain, as seen in the first term on the right side of Eq. 20. This "nonlinear web stress" term is the inverse of the proportional constant from the radial modulus multiplied by the hoop modulus. Thus the inverse proportional constant can be considered as a strain. Typically, this strain is very large, and the resultant stress dominates the web stress. The stress from the nonlinear term is added to the web stress, so the radial stress in the roll is not directly proportional to the web stress. The stress solution in Eq. 21 has assumed a radial modulus exactly proportional to the stress. This means that log(stress) is proportional to the strain for stacked sheets of media. However, original nonlinear stress–strain data do not always support this suggestion. Thus, valid values of α are particularly difficult to obtain, and existing constitutive relations for stacked media are often inadequate *(17)*.

The constants that describe the roll media used throughout this paper have all been from loading curves. The analysis throughout is based on the conversion of strains into stress in the roll while unloading. Unloading or relaxation of the strains in the web are assumed to be equivalent to loading stresses in all elastic solutions, even when nonlinear. However, experimental results show very large differences between loading and unloading stress-vs.-strain curves in stacked sheets. The web strains are from loading, and the roll stresses are from unloading. In elastic materials, these are easily connected, but in layered media, hysteresis gives differences between loading and unloading curves. In the context of the proposed model, the elastic compliances from unloading are more appropriate when finding the stresses in center-wound rolls. **TJ**

Burns is a professor of mechanical engineering and materials science; Meehan is a materials engineer; and Lambropoulos is a professor of mechanical engineering and materials science in the Materials Science Program, Department of Mechanical Engineering, University of Rochester, Rochester, NY 14627-0133.

Support from the National Science Foundation through the University of Rochester's Center for Optoelectronics & Imaging is appreciated. Thanks also to Zig Hakiel, Larry Fisher, Dick Benson, John LaFleche, and Gary Conners for helpful discussions. Finally, thanks to Larry Fisher, who kindly provided an advance copy of his paper with the supporting data.

Received for review July 27, 1998.

Accepted Jan. 15, 1999.

NOMENCLATURE

a = hub radius
A = arbitrary constant
B = arbitrary constant
C = ratio of elastic properties
D = $r(d/dr)$
E_c = hub core stiffness, GPa
E_r = radial modulus
M = hub torque
r = roll radius ratio, dimensionless
R = outer roll radius ratio
s_{ij} = elastic compliances
s_{11} = radial elastic compliance
s_{22} = hoop elastic compliance
s_{23} = Poisson's elastic compliance = $-\nu s_{22}$
s_{33} = z-axis elastic compliance = s_{22}
t = integration variable
T = tension
u = radial displacement
α = nonlinear radial coefficient
β = see Eq. 9
ε_{ij} = elastic strains
ε^*_{ij} = residual strains
ν = Poisson's ratio of web
σ_{ij} = stresses
σ_w = web stress
σ_{rr} = radial stress
$\sigma_{\theta\theta}$ = hoop stress
σ^* = effective residual web stress

LITERATURE CITED

1. Altmann, H. C., *Tappi* 51(4): 176(1968).
2. Boutaghou, Z-E. and Chase, T. R., *J. Appl. Mech.* 58: 836(1991).
3. Yagoda, H. P., *J. Appl. Mech.* 47: 847(1980).
4. Pfeiffer, J. D., *Tappi* 62(10): 83(1979).
5. Hakiel, Z., *Tappi J.* 70(5): 113(1987).
6. Good, J. K., Pfeiffer, J. D., and Giachetto, R. M., *1992 Web Handling Symposium Proceedings*, AMD-Vol. 149, ASME Applied Mechanics Division, New York, pp. 1–12.
7. Zabaras, N., Liu, S., Koppuzha, J., *et al.*, *J. Appl. Mech.* 61: 290(1994).
8. Benson, R. C., *J. Appl. Mech.* 62: 853(1995).
9. Olive, G. A., "A study of wound rolls during winding and unwinding," MS thesis, Dept. of Mechanical Engineering, University of Rochester, Rochester, NY, 1994.
10. Chang, Y. B., Chambers, F. W., and Shelton, J. J., *J. Tribology* 118: 623(1996).
11. Boyce, W. E. and DiPrima, R. C., *Elementary Differential Equations and Boundary Value Problems*, John Wiley & Sons, New York, 1965, pp. 119–121.
12. Pfeiffer, J. D., *Tappi* 49(8): 342(1966).
13. Pfeiffer, J. D., *Tappi* 51(8): 77(1968).
14. Qualls, W. R. and Good, J. K., *J. Appl. Mech.* 64: 871(1997).
15. Koppuzha, J. K., *Adv. Info. Storage Systems* 4: 73(1992).
16. Fisher, L. W., *Case Studies in Mechanical Engineering Design: Proceedings of 1998 ASME International Congress and Exposition*, ASME, New York, Paper No. 98-WA/DE-1.
17. LaFleche, J., unpublished data, Materials Science Laboratory, University of Rochester, NY, 1995.